Seismic performance analysis of self-centering steel frames with intermediate columns containing friction dampers

Zhang Yanxia, Chen Yuanyuan, Zhao Wenzhan & Wang Zongyang

Beijing Higher Institution Engineering Research Center of Structural Engineering and New Materials,School of Civil and Transportation Engineering, Beijing University of Civil Engineering and Architecture, Beijing 100044, China.

ABSTRACT: A self-centering steel frame system with intermediate columns containing friction dampers (ICSCSF) has been proposed in this study for using in seismically active regions and in larger span self-centering steel structures. An eight-floor, ICSCSF was designed, and pseudo-dynamic test was conducted on a two-floor plane sub-structure. This paper presents a finite element model using ABAQUS to investigate the dynamic mechanical behavior of ICSCSF compared with the pseudo-dynamic test results. The experimental and FEA results indicated that the introduction of intermediate columns containing friction dampers greatly increased the lateral stiffness of the structure and that the friction dampers were capable of dissipating the energy of medium-and high-magnitude seismic activity. The results obtained by finite element analysis are basically consistent with those of the test, and the feasibility of the finite element numerical simulation was verified. This is workable method to forecast the mechanical performance of this structure system before pseudo dynamic test in the future.

KEYWORDS： Self-centering steel frame; Intermediate columns; Friction damper; Pseudo-dynamic test; finite element analysis

1 INTRODUCTION

Conventional moment resisting frames (MRFs) are designed to dissipate energy under the design earthquake by developing yielding and damage in critical regions of the main structural members. This damage can result in large residual drift after the earthquake. A self-centering moment resisting frame (SC-MRF) is proposed(Ricles et al 2001) to reduce the main structural damage, reduce or eliminate residual drift, and is easy to repair after a strong earthquake (Garlock et al 2003; Kim et al 2008; Iyama et al 2009; Wolski et al 2009). However, when a self- centering steel frame structure is located in a seismically active region or its span is relatively large, it is difficult to satisfy the design requirements because of the relatively low stiffness and the large story drift response. A prestressed steel frame system with intermediate columns containing friction dampers (simply referred to ICSCSF) has been proposed. An 3×5-bay, 8-story, ICSCSF prototype building was designed. A 0.4-scale 1-bay, 2-story sub-structure of the ICSCSF was developed and pseudo-dynamic test was conducted. This paper presents a finite element model using ABAQUS to investigate the dynamic mechanical behavior of ICSCSF compared with the experimental results. This is workable method to forecast the mechanical performance of this structure system before pseudo dynamic test in the future.

2 DETAILS OF THE ICSCSF

The ICSCF consists of post-tensioned (PT) strands , bolted web friction devices （WFDs） connections (Tsai et al 2008; Lin et al 2013; Zhang,A.L. et al 2013; Zhang,Y.X. et al 2014) and intermediate columns, is shown in Figure 1(a). The beams are connected to the column through two beam web FDs. Each FD consists of two web clamping plates welded to the column flange and connected to the beam web using energy dissipatting bolts. Brass plates are sandwiched between the webs of the beam and the clamping plates to achieve reliable friction and dissipate energy.PT strands run along two sides of the beam web and run through the column flanges. The design principle is to enable the connection to develop a gap opening at the beam-column interface, and the PT force enables the connection to self-center upon unloading. Thus, the energy dissipation occurs in special

devices designed for the beam-column connection regions.The upper intermediate column, the lower intermediate column, and the friction damper (Japan 2008) composed the intermediate columns.The upper and lower intermediate columns are fixed on the beams or column base. The upper and lower intermediate columns are connected through the friction damper. The friction damper details are shown in Figure 1(b),the damper includes a T-shaped plate and two L-shaped connected to the upper intermediate column and the lower intermediate column, respectively, by energy dissipatting bolts to enable easy replacement of the damper following an earthquake. In addition, there are brass plates sandwiched in the L-shaped and T-shaped plates. An elongated hole in the T-shaped plate allows the upper and lower intermediate columns to move relative to one another in an earthquake, and dissipating energy by friction. Pseudo-dynamic tests were conducted on the two-floor (floors 1 and 2) experimental substructure with intermediate columns and six-floor (floors3–8) analytical substructure without intermediate columns. The tested schematic and photograph are shown in Fig2. and Fig.3. In the tests, axial compression is supplied by two 100ton jacks above the columns.;lateral forces are supplied by two 200ton actuators.Simulations of the structural response to a seismic disturbance were used to determine the actuator displacements.

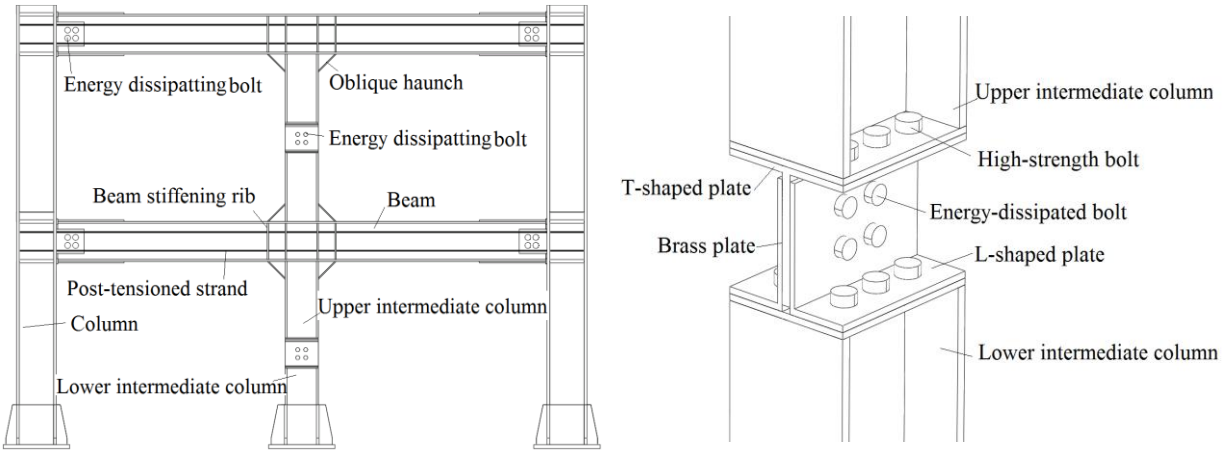

(a) Tested frame (b) Details of the friction damper

Fig. 1 Self-centering steel frame with intermediate column containing friction damper

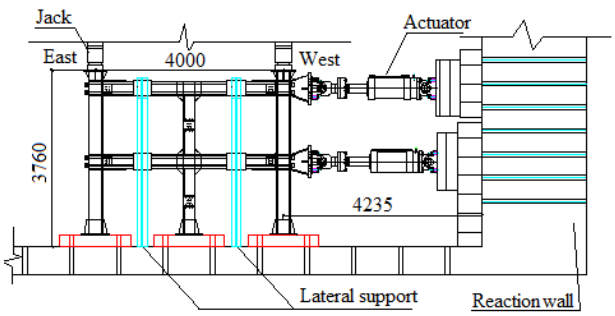

Fig.2 Test schematic

Fig.3 Test photograph

3 FINITE ELEMENT ANALYSIS(FEA)

3.1 *Construction of a finite element model*

3.1.1 *Dimensions of the ICSCSF model*

The structural plan of ICSCSF prototype is shown in Figure 4. There are 3×5-bays, where all spans were 10m. The height of the first floor was 3.9m, and the height of floors 2 to 8 were 3.6m. The red sections are the prestressed steel frame structure with intermediate column (only constructed at floors 1-2); the other parts are hinge systems.The arrangement of the energy dissipating bolted connection is shown in Figure 5. The red sections are the energy dissipating bolted connection. The ICSCSF model member sizes are scaled down from the prototype structure and same as the experimental dimensions.

The height of the first floor was 1.68m, the heights of the remaining floors were 1.56m, and the spans were 4m. The model had H300mm×300mm×16mm×20mm columns,H300mm×200×mm×12mm×14mm frame beams, and H250mm×200mm×12mm×14mm intermediate columns. The beam stiffening ribs and the oblique haunch plates were 10mm thick. To dissipate energy, four 10.9 grade M20 and four 10.9 grade M16 energy dissipatting bolts were used in the energy dissipatting bolted connections and intermediate column friction dampers. The post-tensioned strand was the 1×19 type with a nominal tensile strength of 1860MPa, and the initial force was 30% of the tensile limit ($0.3T_u$).

3.1.2 *Unit selection and mesh generation*

The main body of the ICSCSF finite element model is using C3D8R solid element, and post-tensioned strand using T3D2 truss unit. To give consideration to both calculation accuracy and computational efficiency, approximate global size of grid seeds of shear plate is 12mm, column is 60mm, intermediate column and beam is 40mm, and post-tensioned strand is 80 mm. the mesh generation of the ICSCSF model is shown in Figure 5.

3.1.3 *Geometric and material nonlinearities*

The impact of geometric and material nonlinearities was considered in the model calculation. The steel material used for the test specimens was Q345B. The elastic property of the steel was defined by the elastic modulus(E) and Poisson ratio(ν), while the plastic property data were given in the form of the stress-strain curve. According to the material test data, $E=2\times10^5$MPa and ν=0.3 were used. The PT strand was in the elastic state, and thus, only the elastic modulus and Poisson ratio were defined.

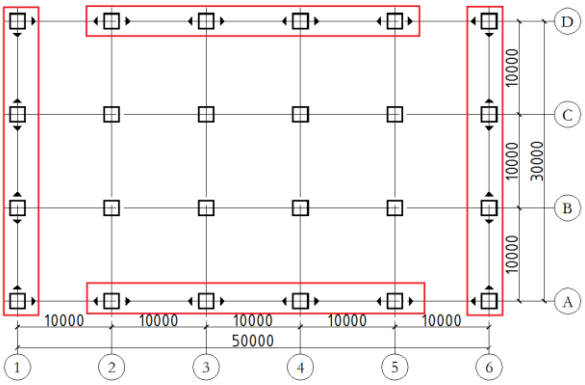

Fig.4 Structural plan of prototype structure

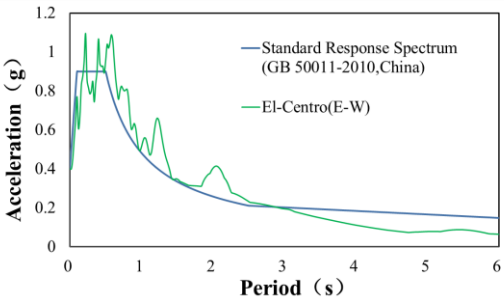

Fig. 6 Acceleration response spectra

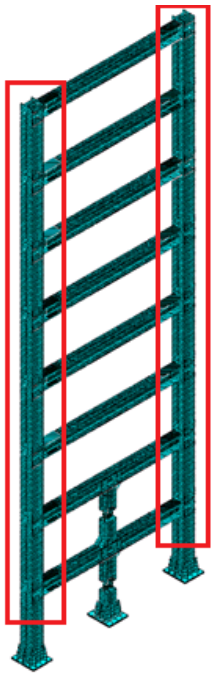

Fig. 5 The mesh generation of the ICSCSF model

3.1.4 *Establishment of pre-tensile force of the high strength bolt and PT force*

The bolt pre-tensile force of the energy dissipatting bolt simulated by using Bolt Load was put on the middle face of screw, and keep it in the whole process of loading. The PT force of strands was simulated by using truss unit, that can only sustain tension except the pressure. The PT force can be achieved by applying the predetermined temperature load to the PT strand, which was defined its linear expansion coefficient in the material properties and initial temperature in the initial analysis step.

3.1.5 *Contact nonlinear*

The interaction between the surface of clamping plate and beam web, T-shaped and two L-shaped plates in the intermediate columns was simulated by defining the friction coefficient in the tangential friction contact and normal hard contact. The coefficient of friction between the brass and steel plates was determined through testing to be 0.34.

3.1.6 *Boundary and load conditions*

The boundary and load conditions are diffrent from the test. In the finite element model,the six degree of freedom at the bottom of the columns are all fixed. To exert acceleration time history upon the ICSCSF finite element model directly to investigate the seismic behavior of the ICSCSF.Seismic data from the El-Centro (E-W) earthquake ground motions were used in the finite element numerical simulation same as the pseudo-dynamic tests. The acceleration response spectra of the ground motions are given in Figure 6. The time step for the El-Centro (E-W) data was was scaled to 0.0063s. The simulation used 5% damping ratio.The Rayleigh damping coefficient alpha and beta are calculate by using the natural frequency of the structure and the damping ratio and defined in the finite element model. Peak values from the seismic acceleration record of 0.07g, 0.2g, 0.4g, 0.51g and 0.62g, correspond to the specifications for the 8-degree frequent, fortification, rare, 8-degree rare(0.3g), and 9-degree rare earthquakes, respectively, according to Chinese Code for Seismic Design of Buildings(GB 50011-2010,2010), were chosen as the inputs for the FEA.

3.2 *Comparison of the ICSCSF FEA and test results*

3.2.1 *Displacement response*

Finite element analysis of the tested ICSCSF was conducted. Test and FEA comparison of floor displacement time histories of from El-Centro ground motion (0.4g and 0.62g) are shown in Figure 7. Comparison of the maximum floor displacement and story drift are shown in Table 1.

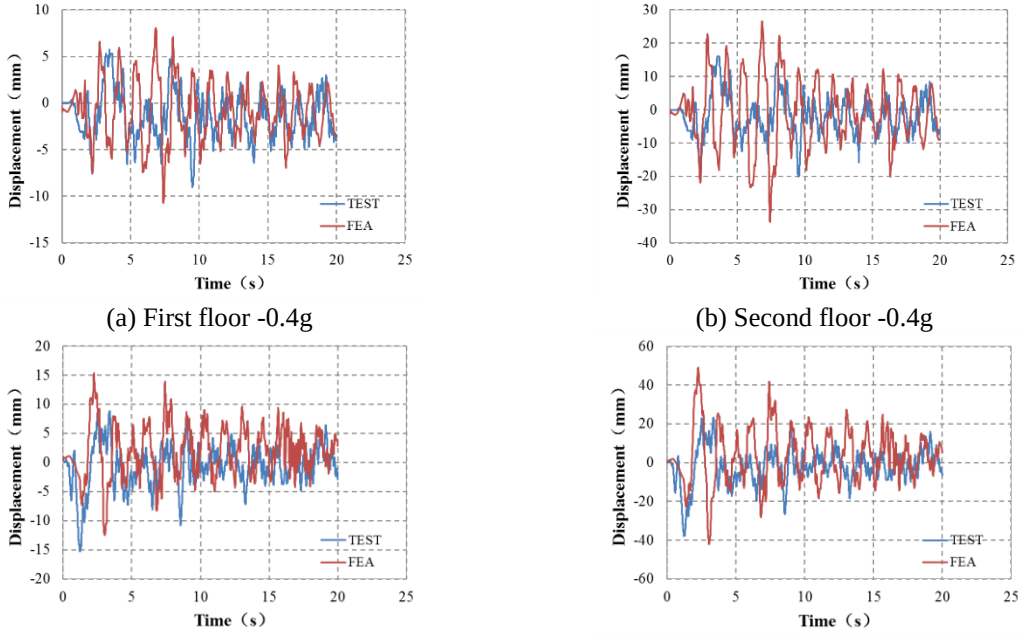

(a) First floor -0.4g (b) Second floor -0.4g

(c) First floor -0.62g (d) Second floor -0.62g

Fig.7 Test and FEA comparison of floor displacement time histories from El-Centro

As can be seen from the figure 7 and table 1, when the peak seismic acceleration increased to 0.4g, the maximum lateral displacements of test and FEA of first floor were 9.05mm and 10.75mm, respectively,and the second floor were 20.19mm and 33.67mm, respectively. Maximum story drift of the second floor from the test and FEA were 1/141 and 1/68, respectively, under the actions of ground motions with peak accelerations of 0.4g, indicating that the intermediate column friction dampers greatly increased the lateral stiffness of the structure according to the limit of 1/50 under the actions of ground motion of 0.4g(GB 50011-2010,2010). When the peak seismic acceleration increased to 0.62g,

the maximum displacements of test and FEA of first floor were 15.20mm and 15.40mm, respectively, and the second floor were 38.14mm and 48.95mm, respectively. By comparing the finite element analysis results including deformation state with the tests, it shows good agreements between them. The differences boundary and load conditions in test frame and finite element model led to deviation between test and finite element analysis results.

Table 1. Test and FEA comparison of maximum floor displacement and story drift

Seismic peak acceleration		First floor				Second floor			
		Maximum displacement (mm)		Maximum story drift (%rad)		Maximum displace-ment (mm)		Maximum story drift (%rad)	
		Positive	Negative	Positive	Negative	Positive	Negative	Positive	Negative
0.07g	TEST	3.55	-2.88	0.19	-0.15	7.63	-6.52	0.26	-0.23
	FEA	1.75	-0.20	0.09	-0.01	3.58	-1.59	0.09	-0.12
0.2g	TEST	4.5	-5.64	0.24	-0.30	11.83	-12	0.47	-0.41
	FEA	3.95	-2.84	0.21	-0.15	10.54	-9.57	0.43	-0.42
0.4g	TEST	5.75	-9.05	0.31	-0.49	16.52	-20.19	0.69	-0.71
	FEA	10.75	-8.10	0.58	-0.44	33.67	-26.65	1.19	-1.48
0.51g	TEST	7.61	-10.7	0.41	-0.58	20.41	-25.48	0.82	-0.95
	FEA	8.58	-6.70	0.46	-0.36	34.31	-28.46	1.41	-1.68
0.62g	TEST	8.84	-15.2	0.48	-0.82	23.27	-38.14	0.93	-1.47
	FEA	15.40	-12.52	0.83	-0.67	48.95	-41.99	1.90	-2.20

Figure 8 shows the test and FEA comparison of the relative slippage time histories of the intermediate column damper slippage for every floor. Table 2 lists the test and FEA comparison of maximum slippage and residual values.

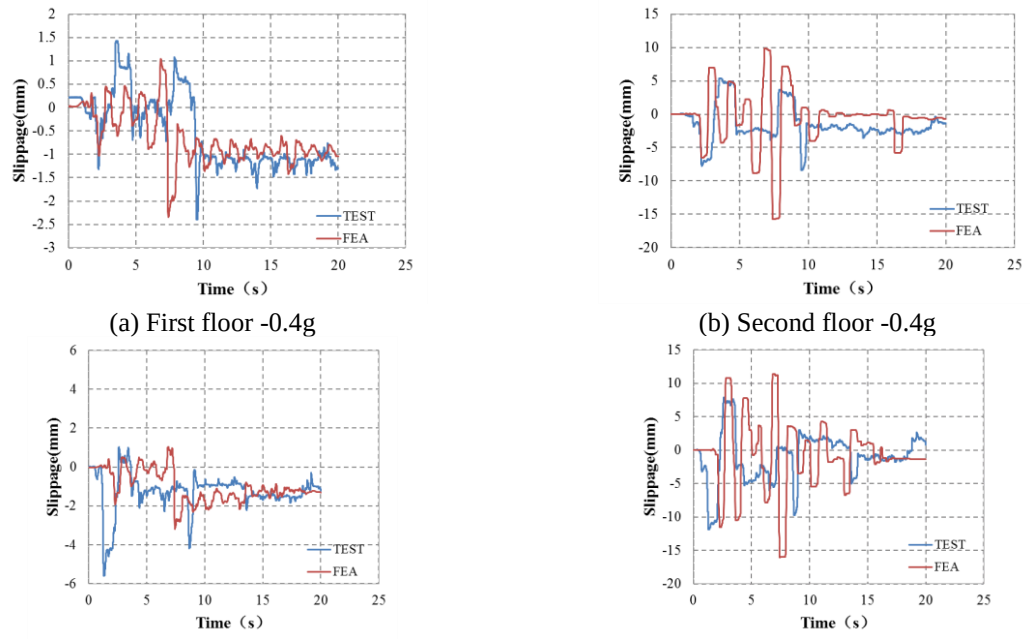

(a) First floor -0.4g (b) Second floor -0.4g

(c) First floor -0.51g (d) Second floor -0.51g

Fig.8 Test and FEA comparison of relative slippage time histories of the friction damper from El-Centro

As can be seen from the figure 8 and table 2, with the increasing of peak seismic acceleration, the damper slippage of the first and second floor gradually increased. The test and FEA maximum damper slippage of first floor reached 13.91mm and 16.03mm,respectively, and second floor reached 21.35mm and 37.16mm, respectively. The test and FEA residual damper slippage is also relatively small, the maximum being of first floor only 3.10mm and 1.77mm,respectively, second floor only 2.360mm and 0.642mm,respectively. The effect on the overall structure properties is limit, and there

was no observable damage to the structure.The above test and finite element analysis results indicate that in the loading process, the finite element simulated deformation process was very close to that of the test results. The differences boundary and load conditions in test frame and finite element model led to deviation between test and finite element analysis results.

Table 2 Maximum and residual friction damper slippage comparison (mm)

Seismic peak acceleration		Maximum friction damper slippage				Residual friction damper slippage	
		First floor		Second floor		First floor	Second floor
		Positive	Negative	Positive	Negative		
0.07g	TEST	0.100	-0.240	0.470	-0.400	0.030	0.040
	FEA	0.005	-0.070	0.006	-0.010	-0.041	-0.003
0.2g	TEST	0.350	-0.570	2.460	-2.280	0.020	1.520
	FEA	0.187	-0.268	0.234	-0.288	-0.041	-0.013
0.4g	TEST	1.420	-2.400	5.390	-8.370	-1.150	-1.140
	FEA	2.338	-1.046	15.741	-9.819	0.943	0.651
0.51g	TEST	1.030	-5.610	7.900	-11.850	-1.010	-0.210
	FEA	3.195	-1.038	16.046	-11.424	1.278	1.358
0.62g	TEST	1.280	-13.910	9.200	-21.350	-3.100	-2.360
	FEA	16.030	-11.430	37.157	-30.088	1.770	0.642

3.2.2 *Hysteresis loop*

Figure 9 shows test and FEA comparison of the hysteresis loops of first floor shear and displacement from EL-Centro. Generally speaking, the hysteresis curves obtained by finite element analysis are basically consistent with those of the test results, indicating that the method adapted in the finite element simulation mainly reflected the real situation of the test. The differences boundary and load conditions in test frame and finite element model led to deviation between test and finite element analysis results.There was no energy dissipation and the test frame remained elastic for the peak accelerations of 0.07g. When the seismic peak acceleration increased to 0.2g, the dampers dissipated energy by sliding and the hysteresis loop started to form, although the enclosed area was relatively small. With the increasing of the peak acceleration, the hysteresis loop enclosed area gradually increased, and the energy-dissipating capacity of the frame became evident, which indicated that the friction damper have a stable energy-dissipating capability.

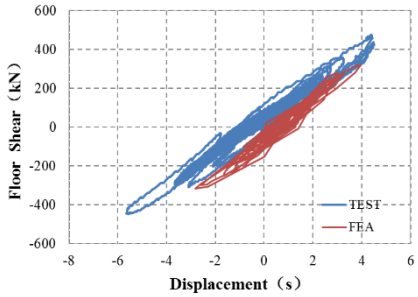

(a)El-Centro-0.2g

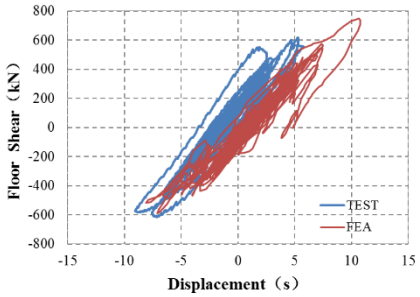

（b）El-Centro-0.4g

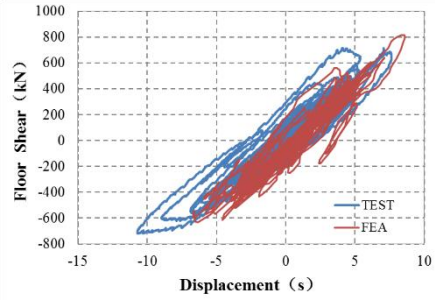

(c)El-Centro-0.51g

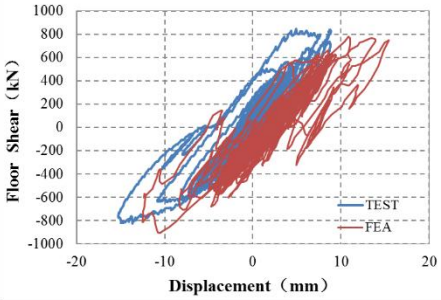

（d）El-Centro-0.62g

Fig.9 Test and FEA comparison of hysteresis loops of floor shear and displacement from El-Centro

3.2.3 *Steel strand PT force*

Test and FEA comparison of PT force time histories for El-Centro record(0.62g) are shown in Figure 10. The maximum PT force of strands are listed in Table 3. It can be observed from the figure that the finite element analysis results is greater than the test results because factors such as the retraction of the core wire in the PT strands and anchor clip plate sliding were not considered. As can be seen from the table 3,there was not obvious variation in the PT force because the column-beam connection gaps in the test frame were relatively small, and the elongation of the strand was relatively small. The decrease in the PT force after the completion of the experiments was small, the PT strand provided an excellent self-centering mechanism.

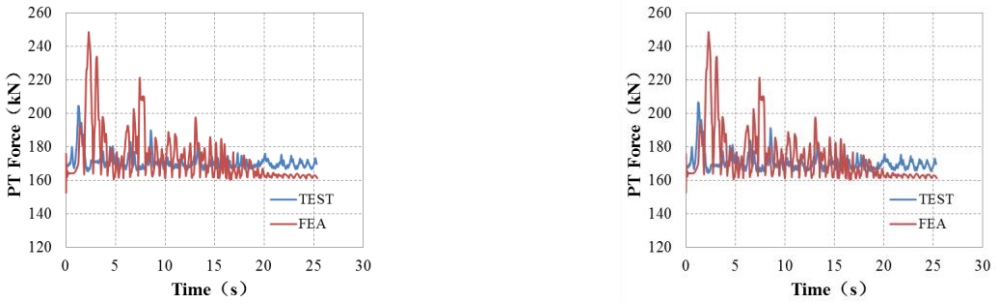

(a) S5-First floor -0.62g (b) S7-Second floor -0.62g

Fig.10 Test and FEA comparison of PT force time histories for El-Centro record

Table 3 Test and FEA comparison of maximum PT force

Maximum PT force			Strand 1	Strand 2	Strand 3	Strand 4	Strand 5	Strand 6	Strand 7	Strand 8
0.07g	TEST	T（kN）	164.24	164.34	184.20	186.60	173.06	177.26	172.89	176.76
		T/T_u	0.28	0.28	0.31	0.32	0.29	0.30	0.29	0.30
	FEA	T（kN）	175.92	175.92	175.92	177.11	176.47	176.47	175.92	177.12
		T/T_u	0.30	0.30	0.30	0.30	0.30	0.30	0.30	0.30
0.2g	TEST	T（kN）	167.87	166.15	187.98	189.34	176.71	181.42	176.64	180.91
		T/T_u	0.28	0.28	0.32	0.32	0.30	0.31	0.30	0.31
	FEA	T（kN）	175.92	175.92	175.92	177.11	176.47	176.47	175.92	177.12
		T/T_u	0.30	0.30	0.30	0.30	0.30	0.30	0.30	0.30
0.4g	TEST	T（kN）	174.46	171.72	194.84	195.10	182.75	188.08	182.68	187.70
		T/T_u	0.30	0.29	0.33	0.33	0.31	0.32	0.31	0.32
	FEA	T（kN）	212.48	212.47	191.78	191.53	211.96	211.95	191.78	191.53
		T/T_u	0.36	0.36	0.32	0.32	0.36	0.36	0.32	0.32
0.51g	TEST	T（kN）	178.76	177.56	198.90	200.17	188.65	194.74	189.80	194.76
		T/T_u	0.30	0.30	0.34	0.34	0.32	0.33	0.32	0.33
	FEA	T（kN）	212.11	212.10	192.76	192.39	212.14	212.14	192.77	192.39
		T/T_u	0.36	0.36	0.33	0.33	0.36	0.36	0.33	0.33
0.62g	TEST	T（kN）	189.79	187.30	210.10	209.08	204.52	210.41	206.57	211.38
		T/T_u	0.32	0.32	0.36	0.35	0.35	0.36	0.35	0.36
	FEA	T（kN）	207.88	206.91	207.88	206.91	248.56	246.14	248.56	246.14
		T/T_u	0.35	0.35	0.35	0.35	0.42	0.42	0.42	0.42

4 CONCLUSIONS

A self-centering steel frame system with intermediate columns containing friction dampers has been proposed and finite element analysis of the ICSCSF pseudo-dynamic tested with ground motions of various degrees was conducted. The following conclusions were drawn:

(1) Displacement response, the friction damper relative slippage and residual damper slippage simulated by the finite element analysis were close to that of the test results. The differences boundary and load conditions in test frame and finite element model led to deviation between test and finite

element analysis results.Both resuls indicated that the intermediate column friction dampers greatly increased the lateral stiffness of the structure,and residual damper slippage are all relatively small.

(2) The hysteresis curves obtained by finite element analysis are basically consistent with those of the test. As the peak acceleration of ground motion increased, the frame dissipated more energy and the area enclosed by the floor shear-displacement hysteresis loops of the floors gradually increased.

(3) The finite element analysis PT force is greater than the test results because factors such as the retraction of the core wire in the PT strands and anchor clip plate sliding were not considered.The PT force variations of the finite element analysis and experiment were the same.The variation of PT force was small, and the decrease in the initial PT force was also small. The PT strand provided an excellent self-centering mechanism for the structure.

(4) In general, comparative analysis of the results from numerical simulation to the experimental results, the feasibility of the finite element numerical simulation was verified. This is workable method to forecast the mechanical performance of this structure system before pseudo dynamic test in the future. The introduction of the friction dampers greatly increased the lateral stiffness of the self-centering steel frame system, and was able to dissipate energy through the sliding action of the friction dampers when subjected to medium-and high-magnitude earthquake ground motion. The self-centering steel frame system with intermediate columns containing friction dampers was fit for using in seismically active regions or larger span self-centering steel structures.

ACKNOWLEDGMENTS

The research reported herein is supported by the National Natural Science Foundation of China under Grant No. 51278027.

REFERENCES:

Garlock M., Ricles J. M., and Sause R. 2003. Cyclic load tests and analysis of bolted top-and-seat angle connections. " J. Struct. Eng., 129(12),1615-1625.

GB 50011-2010. 2010. *Code for seismic design of buildings*. Beijing:China Architecture & Building Press.(in Chinese)

Iyama J., Seo C.Y., Ricles J.M., and Sause R. 2009 . Self-centering MRFs with bottom flange friction devices under earthquake loading. *J. Constr.Steel Res.*.65, 314-325.

Japan association of vibration isolation structure. 2008.*Passive suspension structure design and construction manuals*.Beijing: China Architecture & Building Press.(in Chinese)

Kim H.J., and Christopoulos C. 2008. Friction damped post-tensioned self-centering steel moment-resisting frames. *Journal of Structural Engineering.* 134(11),1768-1779.

Lin Y.C.,Sause R., and Ricles J.M. 2013 . Seismic performance of steel self-centering, moment-resisting frame: hybrid simulations under design basis earthquake. *Journal of Structural Engineering*, 139(11),1823-1832.

Lin Y.C.,Sause R., and Ricles J.M. 2013. Seismic Performance of a Large-Scale Steel Self-CenteringMoment-Resisting Frame: MCE Hybrid Simulationsand Quasi-Static Pushover Tests. *Journal of Structural Engineering*, 139(7),1227-1236.

Ricles J. M.,Sause R.,Garlock M., and Zhao C. 2001. Post-tensioned seismic-resistant connections for steel frames. *Journal of Structural Engineering*.127(2),113-121.

Tsai K.C.，Chou C.C.，Lin C.L.，Chen P.C.，and Jhang S.J. 2008． Seismic self-centering steel beam-to-column moment connections using bolted friction devices.*Earthquake Eng. Struct. Dyn.*, 37,627－645.

Wolski M.,Ricles J.M.,and Sause R. 2009. Experimental study of a self-centering beam–column connection with bottom flange friction device. *Journal of Structural Engineering*, 135(5),479-488.

Zhang A.L.,Zhang Y.X., and Liu X.C. 2013. Research Outlook of Earthquake Resilient Prestressed Steel Structures.*Journal of Beijing University of Technology*, 39(4),507-514. (in Chinese)

Zhang Y.X.,Ye J.J.,Zhao W., Li R., and Liu X.C. 2014. Pushover Study of Self-Centering Plane Steel Frame. *Journal Of Seismiclogical Research*,37(3),475-483. (in Chinese)

Zhang Y.X., Zhang A.L., and Sun W.L. 2014. Behavior Study of Self-Centering Beam-Column Connections in Resilient Steel Frames After Earthquake. *Industrial Construction*, 44（502）,160-167. (in Chinese)